

AD/A-003 454

SOURCE DISTRIBUTION OF TURBULENT BURSTS
DURING NATURAL TRANSITION

Theodore M. Farabee, et al

Naval Ship Research and Development Center
Bethesda, Maryland

August 1974

DISTRIBUTED BY:

NTIS

National Technical Information Service
U. S. DEPARTMENT OF COMMERCE

**BLANK PAGES
IN THIS
DOCUMENT
WERE NOT
FILMED**

UNCLASSIFIED

SECURITY CLASSIFICATION OF THIS PAGE (When Data Entered)

REPORT DOCUMENTATION PAGE		READ INSTRUCTIONS BEFORE COMPLETING FORM
1. REPORT NUMBER SAD-89E-1942	2. GOVT ACCESSION NO.	3. RECIPIENT'S CAT. LOG NUMBER A2/A-003454
4. TITLE (and Subtitle) Source Distribution of Turbulent Bursts During Natural Transition Final		5. TYPE OF REPORT & PERIOD COVERED Final
		6. PERFORMING ORG. REPORT NUMBER
7. AUTHOR(s) Theodore M. Farabee Mario J. Casarella Fred C. DeMetz		8. CONTRACT OR GRANT NUMBER(s)
9. PERFORMING ORGANIZATION NAME AND ADDRESS Naval Ship Research and Development Center Bethesda, Md. 20084		10. PROGRAM ELEMENT, PROJECT, TASK AREA & WORK UNIT NUMBERS Subproject SF43.452.702.06 Task 01356, Work Unit 1942-024
11. CONTROLLING OFFICE NAME AND ADDRESS Naval Sea Systems Command Washington, D.C. 20362		12. REPORT DATE August 1974
		13. NUMBER OF PAGES 52
14. MONITORING AGENCY NAME & ADDRESS (if different from Controlling Office)		18. SECURITY CLASS. (of this report) UNCLASSIFIED
		15a. DECLASSIFICATION/DOWNGRADING SCHEDULE
16. DISTRIBUTION STATEMENT (of this Report) Approved for Public Release: Distribution Unlimited		
17. DISTRIBUTION STATEMENT (of the abstract entered in Block 20, if different from Report)		
18. SUPPLEMENTARY NOTES Reproduced by NATIONAL TECHNICAL INFORMATION SERVICE U S Department of Commerce Springfield VA 22151		
19. KEY WORDS (Continue on reverse side if necessary and identify by block number) Boundary layer transition Turbulent bursts Boundary layer pressure field Turbulent spots Flow noise Hydroacoustic Intermittent transition boundary layer Flat plate transition Intermittent pressure field		
20. ABSTRACT (Continue on reverse side if necessary and identify by block number) The basic statistical properties of the wall pressure field associated with turbulent spots in a transition boundary layer have been measured on a large flat plate test fixture in the Anechoic Flow Facility at the Naval Ship Research and Development Center. The measured statistical properties and the distribution of the turbulent spots on the plate surface are compared with a quantitative formulation of the transition process which was developed by Emmons ^{1,2} . An important unknown parameter in Emmons' model of the transition		

UNCLASSIFIED

SECURITY CLASSIFICATION OF THIS PAGE(When Data Entered)

20.

process is the burst source rate density function. This paper considers the consistency between the predicted and measured statistical burst properties when two simple forms of the source rate density function are assumed. Experimental values of the burst rate and average burst length are presented as a function of the intermittency factor. The statistical results are normalized in term of spatial and temporal individual burst properties and compared with the predicted results.

19.

Intermittent signals from pressure transducers
Burst properties
Intermittency factor
Pressure field measurements
Pressure field bursts
Natural transition
Turbulent burst sources
Burst source rate density function
Transition region width

ia

UNCLASSIFIED

SECURITY CLASSIFICATION OF THIS PAGE(When Data Entered)

TABLE OF CONTENTS

	Page
ABSTRACT	1
ADMINISTRATIVE INFORMATION	1
INTRODUCTION	2
EMMONS' MODEL	3
INTERMITTENCY FACTOR	5
BURST RATE FREQUENCY	7
AVERAGE BURST PERIOD	8
SOLUTIONS FOR PARTICULAR SOURCE FUNCTIONS	11
CASE 1 - $g(x)$ DELTA FUNCTION	11
CASE 2 - $g(x)$ UNIFORM SOURCE DISTRIBUTION	12
EXPERIMENTAL RESULTS	14
COMPARISON OF EXPERIMENTAL RESULTS WITH EMMONS' MODEL	15
DISCUSSION AND CONCLUSIONS	15
ACKNOWLEDGMENT	18
APPENDIX A - DERIVATION OF THE INCREMENTAL VOLUME ELEMENT	29
APPENDIX B - MEASUREMENT OF INTERMITTENT PRESSURE FIELD PROPERTIES.	32
APPENDIX C - METHOD OF NORMALIZATION OF THE DATA	34
REFERENCES	44

10

LIST OF FIGURES

		Page
Figure 1	Relationship Between the Domain of Dependence of a Point P and the Domain of Influence of a Point P_0 (Burst Origin)	19
Figure 2	Measured Properties of Wall Pressure Bursts	20
Figure 3	Intermittency Distribution through the Transition Region	21
Figure 4	Burst Rate Versus Intermittency Factor	22
Figure 5	Average Burst Length Versus Intermittency Factor	23
Figure 6	Comparison of Experimental Data with Emmons' Theoretical Model ($g = n\delta(x-x_t)$)	24
Figure 7	Comparison of Experimental Data with Emmons' Theoretical Model ($g=\text{constant}$)	25
Figure 8	Magnitude of the Source Rate Density n , and the Width of the Transition Region Δx_t	26
Figure 9	Magnitude of the Source Rate Density g , and the Width of the Transition Region Δx_t	27

LIST OF TABLES

Table 1	Emmons' Probabilistic Model	28
---------	-----------------------------	----

LIST OF SYMBOLS

A_d	Projection of burst Retrograde Cone on yt -plane
dA	Incremental surface element
f_B, N	Burst frequency = number of bursts/second
f_B	Dimensionless burst frequency
g	Source rate density function
G	Parameter = $-\ln(1-\gamma)$
n	Number of burst sources per unit length per unit time
P	position on plate surface
R	Dependence Volume, Reynolds number
t	time
T	sample time
U_c	Burst convection velocity = $1/2 (U_\ell + U_t)$
U_e	Freestream velocity at edge of plate boundary layer
U_g	Burst growth rate = $U_\ell - U_t$
U_ℓ	Leading edge velocity of burst
U_t	Trailing edge velocity of burst
dV	Incremental space-time volume element
x, y	Spatial coordinates on plate surface
x_t	Streamwise coordinate at burst onset
\bar{x}	Normalized streamwise distance from burst onset = $\frac{x-x_t}{\Delta x_t}$
Δx_t	Width of transition bursting region
α	Half angle of burst
γ	Intermittency factor

LIST OF SYMBOLS

ϕ, ψ	Probability of burst detection
σ^*	Burst propagation parameter = $\frac{U_g U_e}{U_c U_t} \tan \alpha$
τ_B	Burst length in seconds
$\bar{\tau}_B$	Average burst length
τ_B	Dimensionless Burst length
ξ_t	Distance downstream from burst origin
ζ	Dummy variable of integration

ABSTRACT

The basic statistical properties of the wall pressure field associated with turbulent spots in a transition boundary layer have been measured on a large flat plate test fixture in the Anechoic Flow Facility at the Naval Ship Research and Development Center. The measured statistical properties and the distribution of the turbulent spots on the plate surface are compared with a quantitative formulation of the transition process which was developed by Emmons^{1,2}. An important unknown parameter in Emmons' model of the transition process is the burst source-rate density function. This paper considers the consistency between the predicted and measured statistical burst properties when two simple forms of the source-rate density function are assumed. Experimental values of the burst rate and average burst length are presented as a function of the intermittency factor. The statistical results are normalized in term of spatial and temporal individual burst properties and compared with the predicted results.

ADMINISTRATIVE INFORMATION

The work reported herein was funded by the Naval Ship Systems Command under Subproject SF 43.452.702.06, Task 01356, Work Unit 1942-024.

¹A complete listing of references is given on page 44.

INTRODUCTION

When a streamlined body moves at high speed through a viscous fluid the laminar boundary layer flow along the surface of the body usually undergoes transition to turbulent flow at some location on the forward nose section of the body. Between the laminar and fully-developed turbulent-flow regions of the boundary layer, a transition region exists over a finite length of the nose in which the flow is observed to be intermittent, that is, patches of turbulent flow occur¹ randomly within the laminar boundary layer region on the surface. Detailed measurements³ have shown that these turbulent bursts grow as they are swept downstream until they merge together forming the fully-developed turbulent boundary layer.

An understanding of the parameters that govern the width of this transition region along with detailed data on the convection and growth properties of the turbulent bursts is essential to the formulation of an appropriate wall pressure field forcing function required for the prediction of the flow induced noise which is transmitted through the structures of the moving body.

The basic properties of the wall pressure field associated with turbulent spots have been measured in detail on a large flat plate in the Anechoic Flow Facility^{4,5,6}(AFF) at the Naval Ship Research and Development Center (NSRDC).

This paper concentrates on describing the statistical properties and distribution of turbulent spots during natural transition on a flat plate and presents a statistical model of a source rate density function initially developed by Emmons¹.

EMMONS' MODEL

In 1951, Emmons first advanced the concept of turbulent burst generation in a laminar boundary layer from his observations in a water-table flow experiment. From visual observations, he concluded that the randomly generated turbulent bursts act independently of each other and uniformly grow as they are swept downstream by the flow. In order to develop a quantitative formulation of the transition process, Emmons assumed the existence of a source-rate density function. This function, $g(x_0, y_0, t_0)$, specifies the rate of production of turbulent point-source bursts per unit area on the surface and is dependent on the position on the surface (x_0, y_0) and time of occurrence (t_0) .

Emmons developed a probabilistic model which related the statistical properties of turbulent bursts for any prescribed form of $g(x_0, y_0, t_0)$. The development of Emmons' model was based on probability theory and his limited data on the growth characteristics of turbulent bursts. New data, obtained in Reference (3), have subsequently clarified the growth properties since Emmons' observations with the simple water-table experiment. A brief outline of the concepts involved with the formulation of this model, as presented by Emmons, will now be given.

Consider a point-source $P_0(x_0, y_0, t_0)$ for the creation of a burst on the body surface. In the x, y, t space, this burst sweeps out a cone-like volume whose shape depends upon the convective and growth properties of individual bursts. This volume which originates upstream at a point source P_0 is called the Propagation Cone and is the domain of influence of a source at $P_0(x_0, y_0, t_0)$.

Now consider a point $P(x, y, t)$ at which a flush-mounted pressure transducer is positioned to monitor the intermittent wall-pressure field. The time record of this pressure field signature will indicate intermittent patches of boundary layer turbulence. The fraction of the total sample time that the boundary layer at a given point P is turbulent is defined as the intermittency factor, γ . In the computation of the intermittency factor, one must add up the burst periods (τ_B) from all bursts originating upstream that pass the point P in the sample time T_{total} . However, one must exclude those portions of overlapping bursts that originate at different upstream locations but coincide within the sampling time.

The locus of all points P_0 which can influence the state of turbulence at point P is a volume upstream called the Retrograde Cone (R). This cone-like volume has propagation rays drawn upstream from P reflecting the domain of dependence of point P . All bursts which pass over the point P must have originated within the dependence volume R . Figure 1 shows the projection of the Propagation and Retrograde Cones on the plate surface.

From the basic concepts of the growth and convective properties of turbulent bursts it is possible to use probability theory to

analytically derive certain statistical relationships between the transition region and the properties of the turbulent bursts. Three such statistical relationships analytically derived by Emmons are the intermittency factor, γ , the average burst period, τ_B , and the burst rate frequency, f_B , which is the frequency at which bursts pass a given point. The derivation of these statistical relationships will now be given.

INTERMITTENCY FACTOR

The probability that a burst originating at P_0 will be detected by a downstream transducer located at P is defined by Emmons¹ as

$$\phi(P, P_0) = \begin{cases} 1 & \text{if } P_0 \text{ is located in Region R of P for } x > x_0 \\ 0 & \text{if } P_0 \text{ is not in Region R of P for } x > x_0 \end{cases}$$

If we let

$$dA_0 = dx_0 dy_0 \quad \text{and} \quad dA = dx dy$$

$$dV_0 = dx_0 dy_0 dt_0 \quad dV = dx dy dt,$$

then we would be tempted to say that the fraction of time that P is turbulent is given as

$$\gamma(P) = \int_R \phi(P, P_0) g(P_0) dV_0 \quad (1)$$

where the region of integration of $\phi(P, P_0) g(P_0) dV_0$ is over the dependence volume R . However, note as previously mentioned that more than one burst can be generated within the Region R such that they will coincide in time t at the transducer position P . For example,

bursts originating at $P_0^1(x_0^1, y_0^1, t_0^1)$ and $P_0(x_0, y_0, t_0)$ when $x_0^1 < x_0$ and $t_0^1 < t_0$ can be detected coincidentally (see Figure 1). For this case, two such bursts coinciding at a point P and time t would be counted separately giving twice the actual value of intermittency. To avoid these burst overlaps, it is assumed that the burst originating nearest the leading edge of the plate will be counted as causing the turbulent burst of length τ_B at the transducer position P since it will be of longer duration and have larger burst length. This is true provided that the burst growth rate, U_g , and burst convection velocity, U_c , are identical for both bursts along their downstream paths.

Now, let $\psi(P, P_0) dV_0$ be the probability that a turbulent burst is detected at point P due to sources in dV_0 at a point P_0 but not because of any sources at $P_0^1(x_0^1, y_0^1, t_0^1)$ with $x_0^1 < x_0$, since the source at P_0 is to be counted only if it is the point-source nearest the leading edge. From this probability function, Emmons concludes that

$$\psi(P, P_0) = [\phi(P, P_0) g(P_0) dV_0] \left[1 - \int_{R^1} \psi(P, P_0^1) dV_0^1 \right] \quad (2)$$

where $g(P_0)$ is again the source-rate density function and R^1 is the region shown in Figure 1. The first term in Equation (2), $[\phi(P, P_0) g(P_0) dV_0]$, represents the fraction of time that bursts will be detected at P due to sources at P_0 . The second term $\left[1 - \int_{R^1} \psi(P, P_0^1) dV_0^1 \right]$, is the fraction of time that no bursts are observed at P due to sources upstream of x_0 . Thus the intermittency, or fraction of the total sample time that bursts are being detected at P is given by

$$\gamma(P) = \int_R \psi(P, P_0) dV_0 \quad (3)$$

Emmons solved the integral equation obtained by substituting Equation (2) into (3) and found

$$\gamma(P) = 1 - \exp\left[-\int_R g(P_0) dV_0\right] \quad (4)$$

Equation (4) gives the relationship between the intermittency factor and the form of the source-rate density function $g(P_0)$. This relationship is solely dependent on the form of $g(P_0)$ and the shape of the dependence volume R .

BURST RATE FREQUENCY

During a sample time T_{total} , point P will be turbulent $T_{total} \int \psi(P, P_0) dV_0$ seconds because of sources in dV_0 . The number of bursts passing P from sources at P_0 in dV_0 is

$$\frac{T_{total} \int \psi(P, P_0) dV_0}{\tau_B(P, P_0)} \geq \frac{T_{total} \int \psi(P, P_0) dV_0}{\tau_{B_{max}}} \quad (5)$$

where τ_B is taken as the burst length measured at $P(x, y, t)$ due to a burst originating upstream at $P_0(x_0, y_0, t)$ and $\tau_{B_{max}}$ is the maximum burst length along the centerline of the burst. When $y = y_0$, the burst erupts along an upstream streamline and the sampled burst length τ_B equals $\tau_{B_{max}}$. However, for the general situation, one cannot distinguish between τ_B , the burst period along an arbitrary section of the wedge-shaped burst and $\tau_{B_{max}}$. Since $\tau_{B_{max}}$ is the only quantity amenable to an analytical formulation, the equations are expressed as inequalities. Reference (4) includes data on the

distribution of burst periods obtained from observations at a fixed position. The total number of bursts per second passing P that originate in the domain of dependence region R is then

$$N(P) = T_{\text{total}} \int_R \frac{\psi(P, P_o) dV_o}{\tau_B} \geq \int_R \frac{\psi(P, P_o) dV_o}{\tau_{B_{\text{max}}}} \quad (6)$$

Thus the frequency at which bursts pass point P is the burst rate frequency given by

$$f_B(P) = \frac{N(P)}{T_{\text{total}}} = \int \frac{\psi(P, P_o) dV_o}{\tau_B} \geq \int_R \frac{\psi(P, P_o) dV_o}{\tau_{B_{\text{max}}}} \quad (7)$$

In terms of the source-rate density function Equation (7) is expressed in the form

$$f_B(P) = \int_R \frac{g(P_o) \exp[-\int_{R^1} g(P_o^1) dV_o^1]}{\tau_B} dV_o \geq \int_R \frac{g(P_o) \exp[-\int_{R^1} g(P_o^1) dV_o^1]}{\tau_{B_{\text{max}}}} dV_o \quad (8)$$

AVERAGE BURST PERIOD

The average burst period (length) is given by

$$\bar{\tau}_B = \frac{\gamma(P) T_{\text{total}}}{N(P)} = \frac{\gamma(P)}{f_B(P)} \quad (9)$$

and can be determined once the values of γ and f_B are known.

As can be seen from these equations, the statistical relationships expressed in Equations (4), (8), and (9) are functions of only the source rate density function, $g(P_o)$, and the growth and convective properties of turbulent bursts. If the source-rate density function

is known and the growth and convective burst properties are measured, it is possible to find at least a numerical solution to Equations (4), (8), and (9).

In the solution to Equations (4), (8), and (9) we may assume, for our simple case of a steady mean flow over a flat plate, that the flow properties are functions of only the streamwise coordinate x . This assumption gives

$$g(P_0) = g(x_0, y_0, t_0) = g(x_0) \quad (10)$$

The integrations in Equations (4) and (8) are performed over the domain of dependence R , thus the incremental volume element dV_0 can be expressed in terms of the growth and convective properties of the individual bursts. This transformation of the incremental volume element is shown in Appendix A and is given as

$$dV_0 = \frac{(x-x_0)^2}{U_e} \sigma^* dx_0 \quad (11)$$

and $\tau_{B_{\max}}$ is given as

$$\tau_{B_{\max}} = \frac{U}{U_c U_t} (x-x_0), \quad (11b)$$

where

U_e = freestream velocity at the edge of the boundary layer

$$\sigma^* = \frac{U}{U_c U_t} \frac{g_e}{e} \tan(\alpha) \quad (11c)$$

$$U_g = U_l - U_t, U_c = 1/2 (U_l + U_t) \quad (11d)$$

U_t = trailing edge velocity of burst

$\tan(\alpha)$ = half angle of burst (see Figure 2)

and U_l = leading edge velocity of bursts

Equations (4) and (8) then become, respectively

$$\gamma(x) = 1 - \exp \left[\frac{-\sigma^*}{U_e} \int_0^x g(x_0) (x-x_0)^2 dx_0 \right] \quad (12)$$

and

$$f_B(x) \geq \tan(\alpha) \int_0^x (x-x_0) g(x_0) \exp \left[\frac{-\sigma^*}{U_e} \int_0^{x_0} g(x_1) (x-x_1)^2 dx_1 \right] dx_0 \quad (13)$$

To apply Equations (12) and (13) to the transition on a flat plate the form of the source-rate density function g must be assumed or deduced.

There are two different approaches by which $g(x_0)$ in Emmons' model may be deduced from experimental data. The first approach is to successively differentiate Equation (12) to obtain the relationship given by Narasimha⁷,

$$g(x) = \frac{U_e}{2\sigma^*} \left[\frac{d^3 G}{dx^3} \right] \quad (14)$$

where $G = -\ln(1-\gamma)$. From this relationship measured values of the intermittency distribution can be used to determine the form of $g(x)$.

The second approach is to assume various forms of $g(x)$ and solve Equations (12) and (13). These analytical results can then be compared

to experimentally measured values of $\gamma(x)$, $f_B(x)$, and $\bar{\tau}_B(x)$. This process allows the determination of that form of $g(x)$ which most closely predicts the turbulent bursts properties.

It must be realized that in the first approach, the third derivative of an experimentally determined distribution must be taken. The merits of such an operation, in view of the accuracy of the data, is highly questionable. Thus the more realistic approach is to use the assumed forms of $g(x)$ to solve the analytical expressions and then compare these results to the experimental results.

SOLUTIONS FOR PARTICULAR SOURCE FUNCTIONS

Enmons' model will now be solved for two assumed forms of $g(x)$.

CASE 1 - $g(x)$ DELTA FUNCTION

The first assumed form of $g(x)$ is that of a Dirac's Delta function,

$$g(x) = n\delta(x-x_t) \quad (15)$$

where n is defined as the number of sources per unit length per unit time along a line located at $x = x_t$ from the flat plate's leading edge and is dependent on the freestream velocity U_e . The physical meaning of this form of $g(x)$ is that all sources of turbulent bursts are located along a line perpendicular to the flow stream. Substitution of Equation (15) into (12), (13) and (9) results in the relations

$$\gamma_1 = 1 - \exp\left[\frac{-\sigma^*n}{U_e} \xi_t\right] \quad (15)$$

$$f_B \geq f_{B_1} = n \tan(\alpha) \xi_t \exp\left[\frac{-\sigma^* n}{U_e} \xi_t^2\right] \quad (17)$$

$$\tau_B = \frac{\gamma(x)}{f_B(x)} \leq \bar{\tau}_{B_1} = \frac{\gamma(x)}{f_{B_1}(x)} \quad (18)$$

where ξ_t is defined as $x - x_t$.

Solving Equation (16) for ξ_t in terms of γ_1 , one obtains

$$x - x_t = \sqrt{\frac{U_e}{n\sigma^*} \ln\left(\frac{1}{1-\gamma_1}\right)}. \quad (19)$$

Equation (19) gives a relationship that defines the distance downstream from the transition point at which a given value of intermittency occurs. This relationship can be used to find the width of the transition bursting region, Δx_t , where Δx_t is defined as

$$\Delta x_t \equiv (x - x_t)_{\gamma=0.99} - (x - x_t)_{\gamma=0.01} \quad (20)$$

By substituting Equation (19) into (20) we get

$$(\Delta x_t)_1 = 2.046 \sqrt{\frac{U_e}{n\sigma^*}}, \quad (21)$$

where it is assumed that U_e is essentially constant over the transition region.

CASE 2 - $g(x)$ UNIFORM SOURCE DISTRIBUTION

As a second simple assumed form of g , g is taken as independent of position on the plate. This condition is expressed by

$$g(x) = g = \text{constant}, \quad (22)$$

where g is defined as the number of sources per-unit surface area per unit time. Although g is independent of x it is dependent on the free-stream velocity U_e . The physical meaning of this form of $g(x)$ is that turbulent burst sources are uniformly distributed within the transition region. Substituting Equation (22) into (12) one obtains the relations

$$\gamma_2 = 1 - \exp\left[\frac{-g\sigma^*}{3U_e} \xi_t^3\right] \quad (23)$$

$$f_B \geq f_{B_2} = g \tan(\alpha) \exp\left[\frac{-g\sigma^*}{3U_e} \xi_t^3\right] \int_0^{\xi_t} \zeta \exp\left[\frac{g\sigma^*}{3U_e} \zeta^3\right] d\zeta \quad (24)$$

$$\tau_B = \frac{\gamma(x)}{f_B(x)} \leq \bar{\tau}_{B_2} = \frac{\gamma(x)}{f_{B_2}(x)} \quad (25)$$

Solving Equation (23) for ξ_t we find that

$$x - x_t = \sqrt[3]{\frac{3U_e}{g\sigma^*} \ln\left(\frac{1}{1-\gamma_2}\right)} \quad (26)$$

and substituting for values of x at which $\gamma_2 = .99$ and $\gamma_2 = .01$ we find that

$$(\Delta x_t)_2 = 1.448 \sqrt[3]{\frac{3U_e}{g\sigma^*}}, \quad (27)$$

where U_e is again assumed to be constant over the streamwise transition width.

In order to predict the width of transition using either Equation (21) or (27), the relationship between the source rate density g and the freestream velocity U_e must be known.

EXPERIMENTAL RESULTS

Measurements were made of the spatial and temporal properties of turbulent pressure bursts in the boundary layer transition region on a flat plate (Appendix B discusses the method by which the spatial and temporal properties of the turbulent pressure bursts were measured). The empirical results presented in this section will be compared with those predicted by Emmons' model in the following section.

Figure 2 shows the three-dimensional shape of individual turbulent bursts determined by Schubauer and Klebanoff³ using hot wire anemometers. The values of the burst parameters shown in the figure were those determined in the present study using flush mounted pressure transducers.

Figure 3 shows the experimental intermittency distributions through the transition region in terms of a normalized Reynolds number.

Figure 4 presents the measured values of burst frequency, f_B , plotted versus γ . Faired lines are drawn through those data points which represent measurements made at the same downstream coordinate.

Figure 5 gives the measured mean burst length as a function of the intermittency factor.

COMPARISON OF EXPERIMENTAL RESULTS WITH EMMONS' MODEL

In order to directly compare the experimental results with those predicted using the different forms of the source rate density function, $g(x)$, in Emmons' model, the measured data are normalized relative to the maximum burst frequency (the normalization details are given in Appendix C). Figures 6 and 7 show the comparison between the experimental data and the theoretical results obtained using, respectively, a Dirac Delta function and a constant for the source rate density function in Emmons' model.

As shown in Appendix C, a functional relationship between the freestream velocity, U_e , and the magnitude of the source rate density function can be determined. Figures 8 and 9 show these relationships for the two cases considered. Also shown in the figures are values of the width of the transition region, Δx_t , calculated using the n versus U_e (Equation (C13)) and g versus U_e (Equation (C23)) relationships and Equations (21) and (27), respectively. The five values of Δx_t shown on each figure were calculated from the corresponding data points relating g and U_e which were calculated using Equations (C13) and (C23) of Appendix C.

DISCUSSION AND CONCLUSIONS

Emmons² developed a probabilistic model of the statistical burst properties for the general case of a source-rate density $g(x)$ being dependent on the downstream spatial location. However, lack of available experimental data did not permit him to examine carefully the explicit nature of this $g(x)$ function except for the case of g

equal to a constant. Emmons attempted to evaluate the constant g by using a few 1/5-second strips of hot-wire records published by Schubauer and Skramstad⁸. Similar calculations were made by the authors using the new data included in this report. The results are shown in Figure 9.

Narasimka⁷ assumed the form of $g(x_0, y_0, t_0)$ to be a Dirac Delta function and evaluated Emmons' equations for the resulting $\gamma(x)$ distribution. From the comparison between experimental data and the theoretically obtained $\gamma(x)$ distribution, Narasimha concluded that the turbulent burst generation process does indeed occur like a delta function source along a line transverse to the flow. It has been found by the authors that the $\gamma(x)$ distribution for the constant source model is very similar to the $\gamma(x)$ distribution for the delta source model. The data shown in Figure 3 was also fitted to a Gaussian Integral Curve. The lack of sensitivity in the $\gamma(x)$ distribution to the various forms chosen for $g(x)$ leads one to conclude that the $\gamma(x)$ distribution should not be used as a criterion for determining the $g(x)$ function.

It should be noted that in the present experiment the streamwise extent of the transition region could not be accurately measured at a given flow velocity due to the use of a limited number of fixed, wall-mounted pressure transducers for detecting the wall pressure bursts in the intermittent transition region. Rather, at a given streamwise position the intermittency was varied from burst onset through fully turbulent flow by varying the flow velocity. As shown in Figure 3, the use of the normalized Reynolds number results in

good collapse of the experimental intermittency distributions determined through the transition region by varying flow velocity at different transducer locations on the plate surface.

An important characteristic of the transition process is the point at which the burst frequency maximizes. In Figures 6 and 7 this point can be seen to be at intermittency values of approximately 0.4 and 0.8 for the Dirac Delta source and the constant source, respectively. The maximization point in the experimental burst frequency curves occurs at an intermittency value of approximately 0.6. This experimentally determined maximum point falls between the two analytically determined values for the uniform and line burst source distributions.

As seen in Figures 6 and 7 the normalized experimental data for the case when the burst generation occurs at a line source is in better general agreement with Emmons' theory than for the case of a uniform source distribution.

Inherent in any analytical model for the burst source distribution is a method for predicting the streamwise width of the transition region. The predicted width of the transition region given by Equations (21) and (27) is seen to depend on the freestream flow velocity U_e (U_e is assumed to be constant over the transition region for the mildly accelerating flow over the plate) and the source-rate densities which are also dependent on U_e . Once the form of the source-rate density, g , is accurately determined from controlled laboratory experiments, the use of the technique utilizing fixed transducers for determining the width of the transition region will be possible for more complicated situations. For example, in transition experiments on models or full-scale vehicles where the streamwise traverse of sensors or maintenance

of constant flow velocity is difficult and the number of fixed sensors is limited, the technique adopted in the present experiment will be useful in determining the transition width.

It is concluded that the source distribution of turbulent bursts is still not firmly established. The present results tend to substantiate Emmons' model for predicting burst statistics in the transition boundary layer, and support the line source model for burst generation. The study indicates that more detailed wind tunnel flat plate measurements are still needed in the form of streamwise surveys of burst statistics at constant flow velocities. New experimental data obtained throughout the entire streamwise extent of the transition region at a fixed flow velocity would overcome the uncertainties of interpretation inherent in the present data, which was obtained by varying flow velocity at a fixed streamwise position.

ACKNOWLEDGMENT

The authors wish to express their appreciation to Mr. John T.C. Shen, Head, Hydro-Acoustics Branch for encouraging this study and to NAVSEA Code SEA 037 for their support.

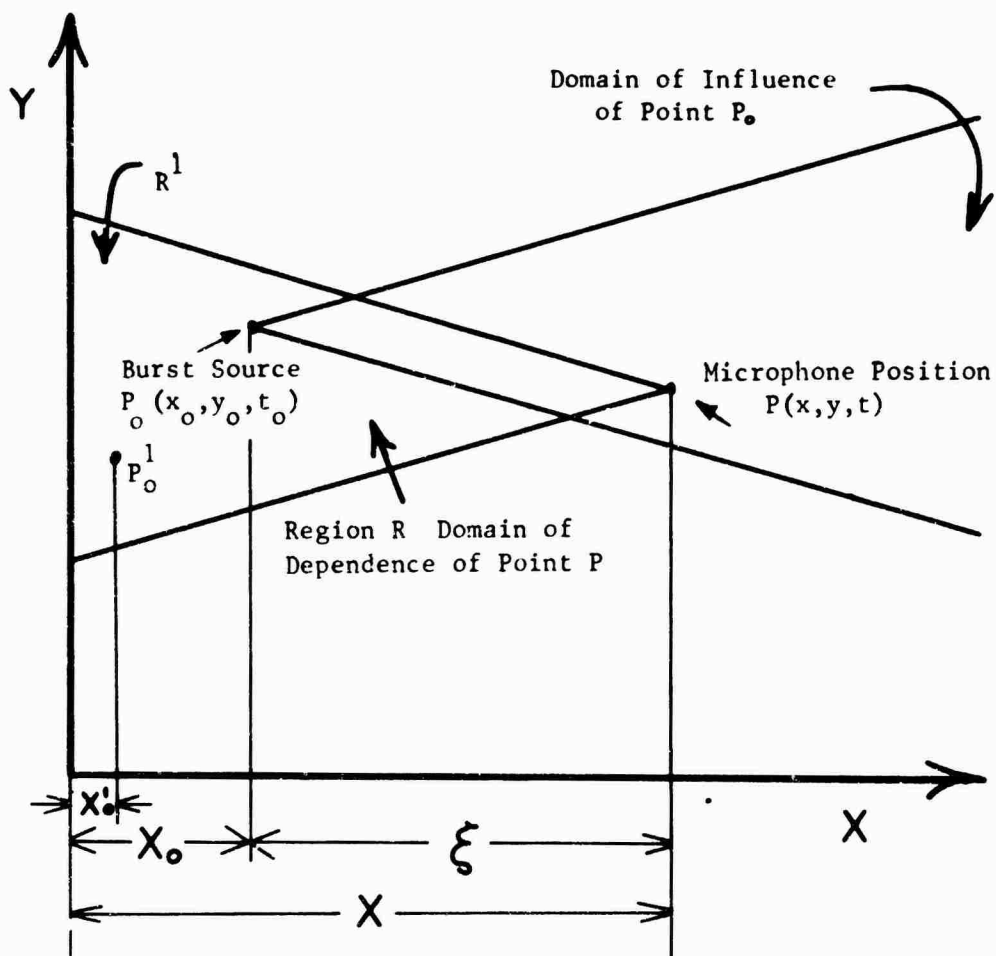


Figure 1 Relationship Between the Domain of Dependence of a Point P and the Domain of Influence of a Point P_0 (Burst Origin)

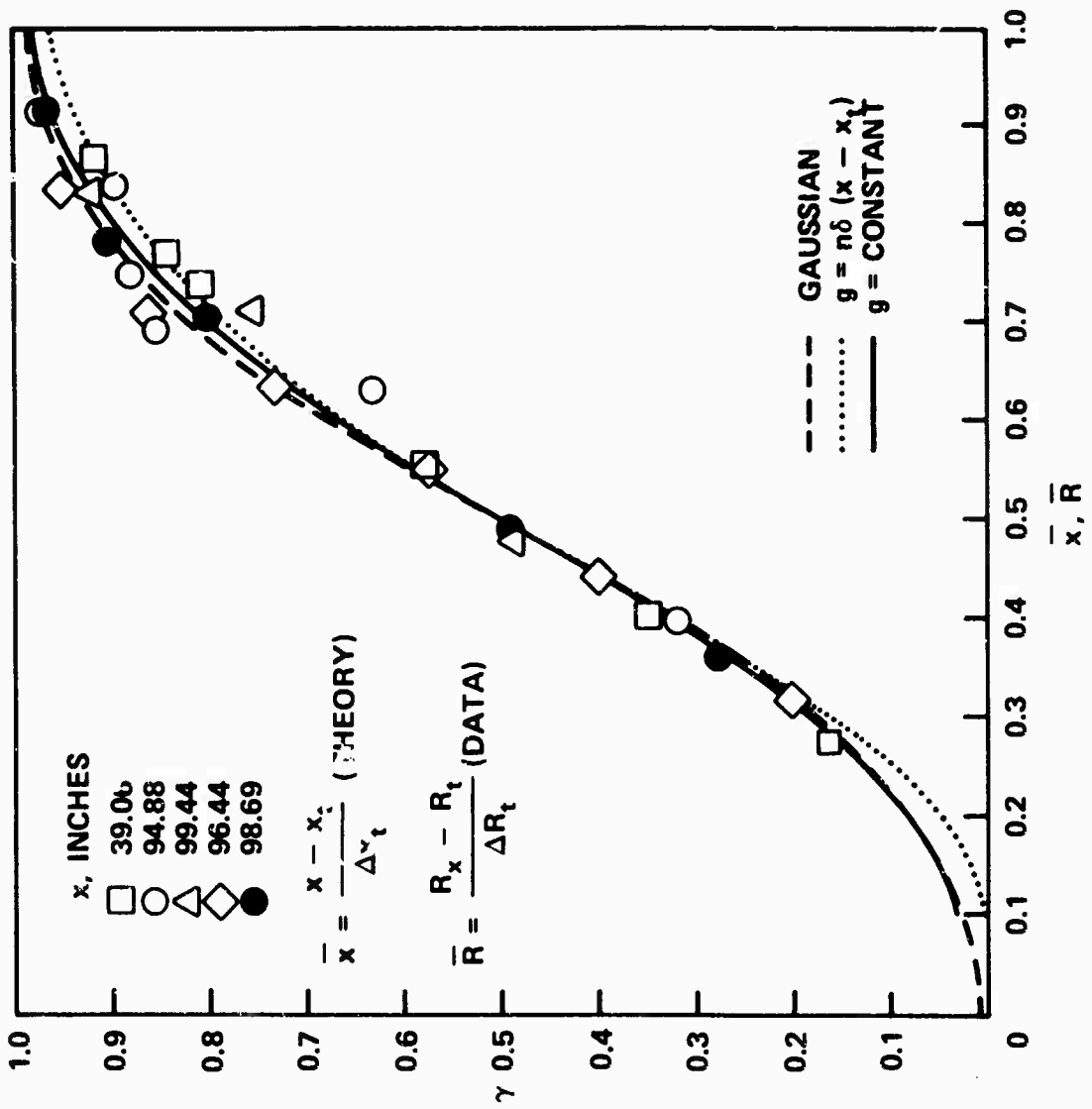
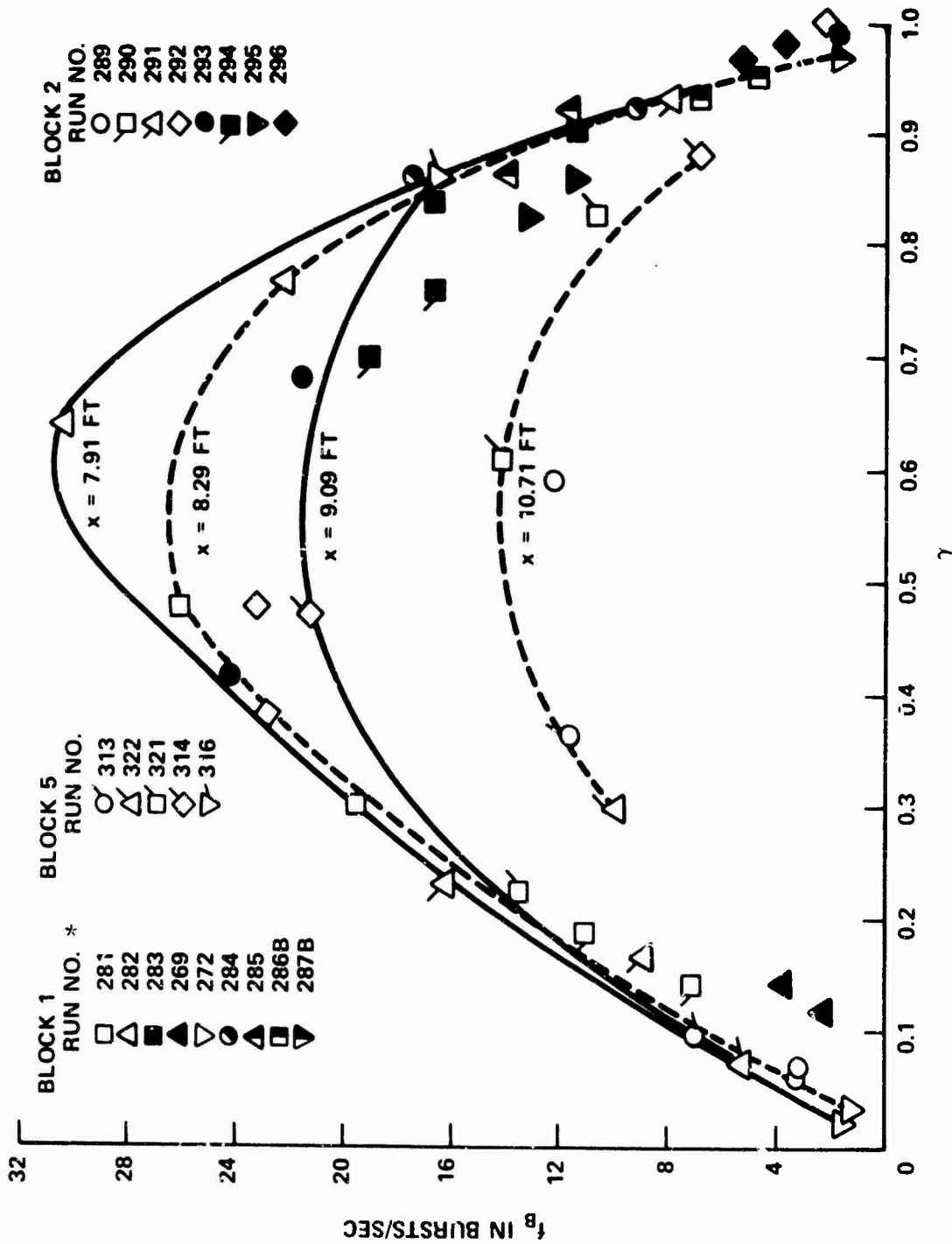


Figure 3 Intermittency Distribution Through The Transition Region



*Run No. relates data to additional flow parameters given in Reference 4

Figure 4 Burst Rate Versus Intermittency Factor

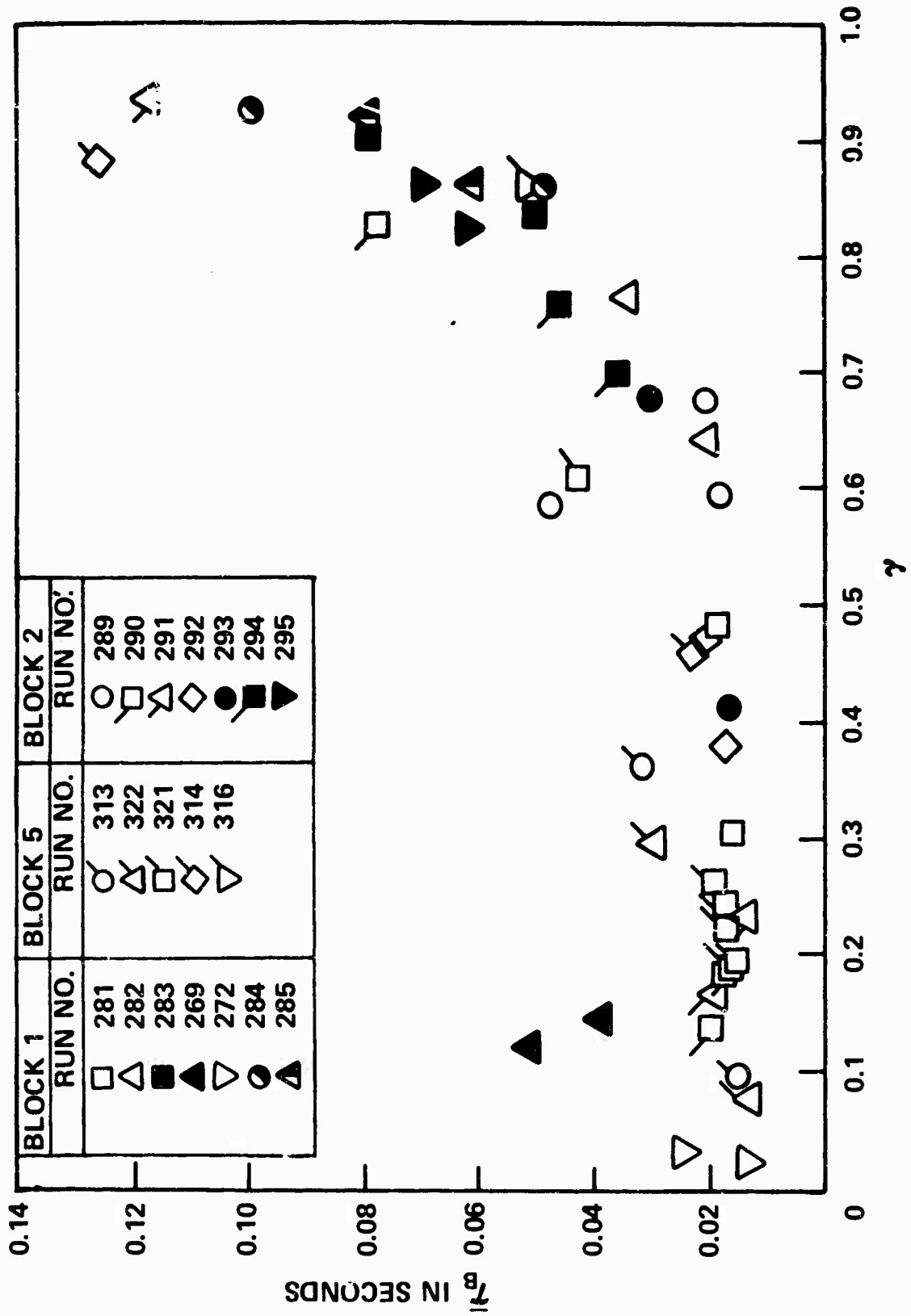


Figure 5 Average Burst Length Versus Intermittency Factor

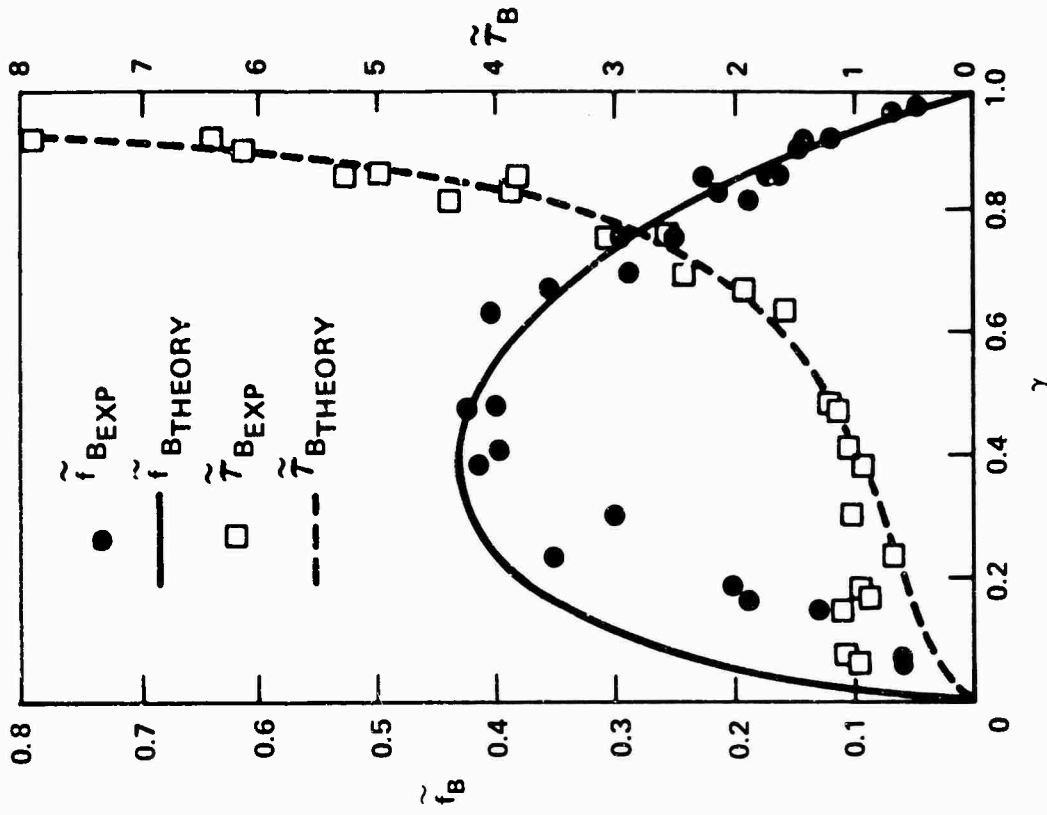


Figure 6 Comparison Of Experimental Data With Eimmons' Theoretical Model ($g = n\delta(x - X_0)$)

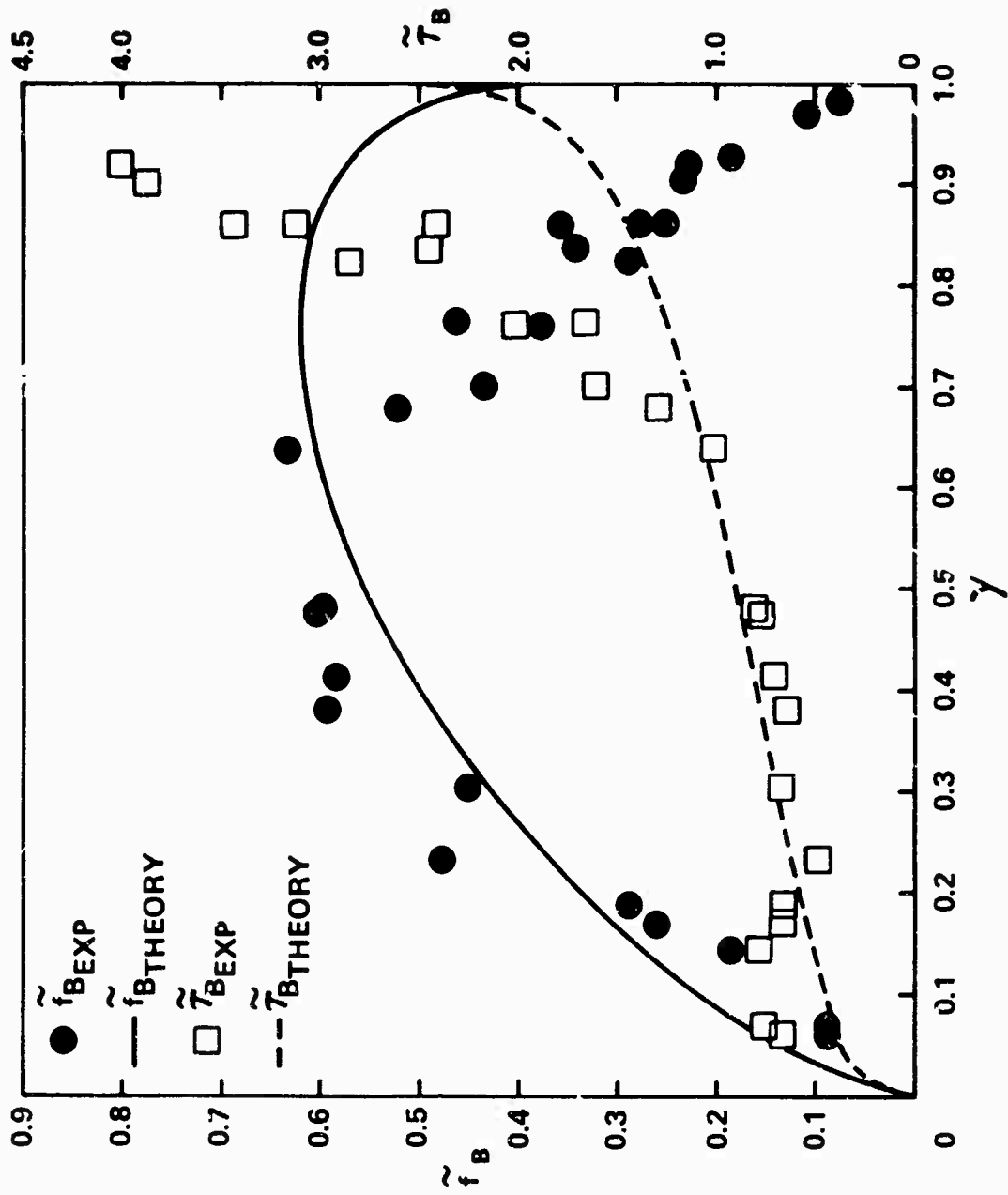


Figure 7 Comparison Of Experimental Data With Emmons' Theoretical Model ($g=\text{constant}$)

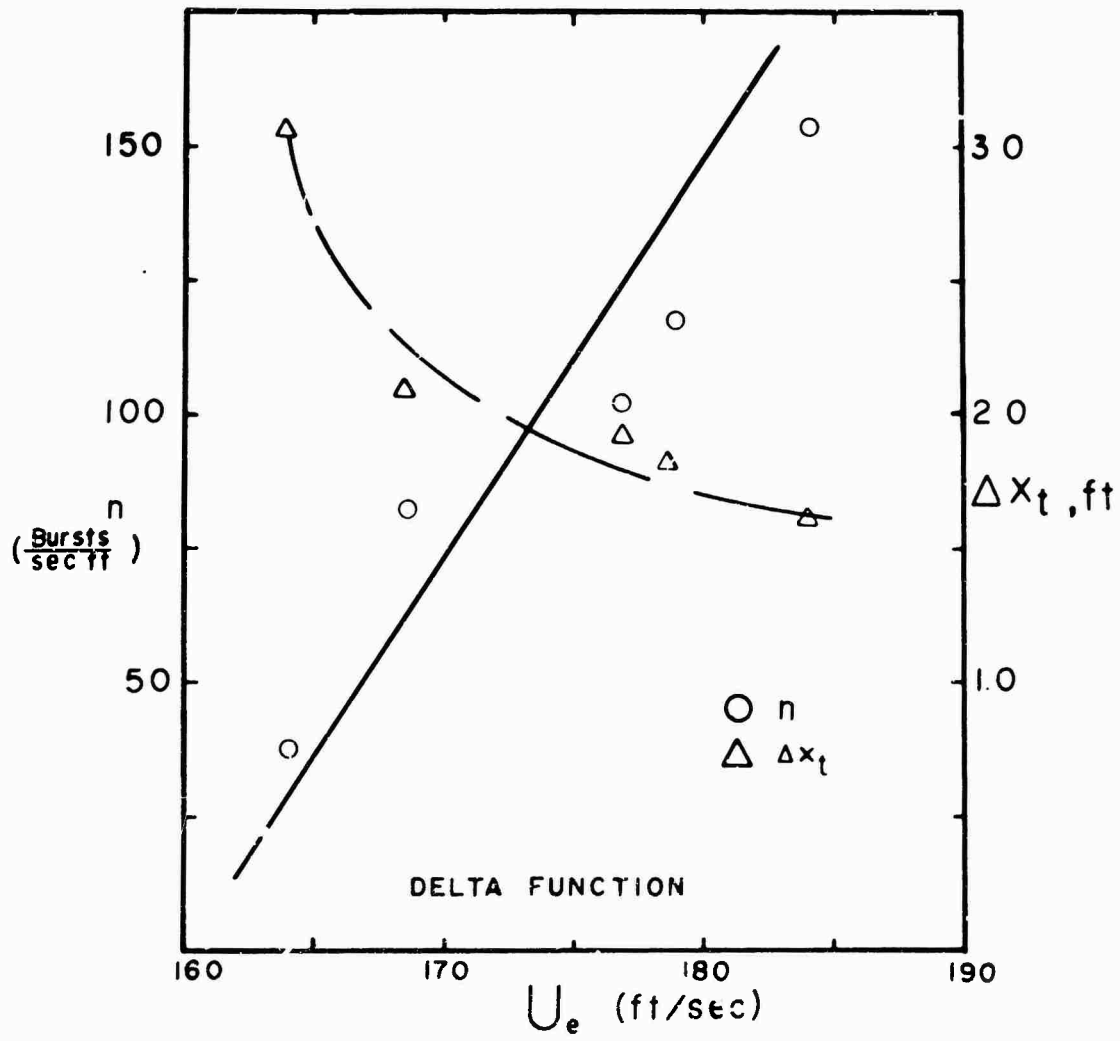


Figure 8 Magnitude of the Source Rate Density n , and the Width of the Transition Region ΔX_t

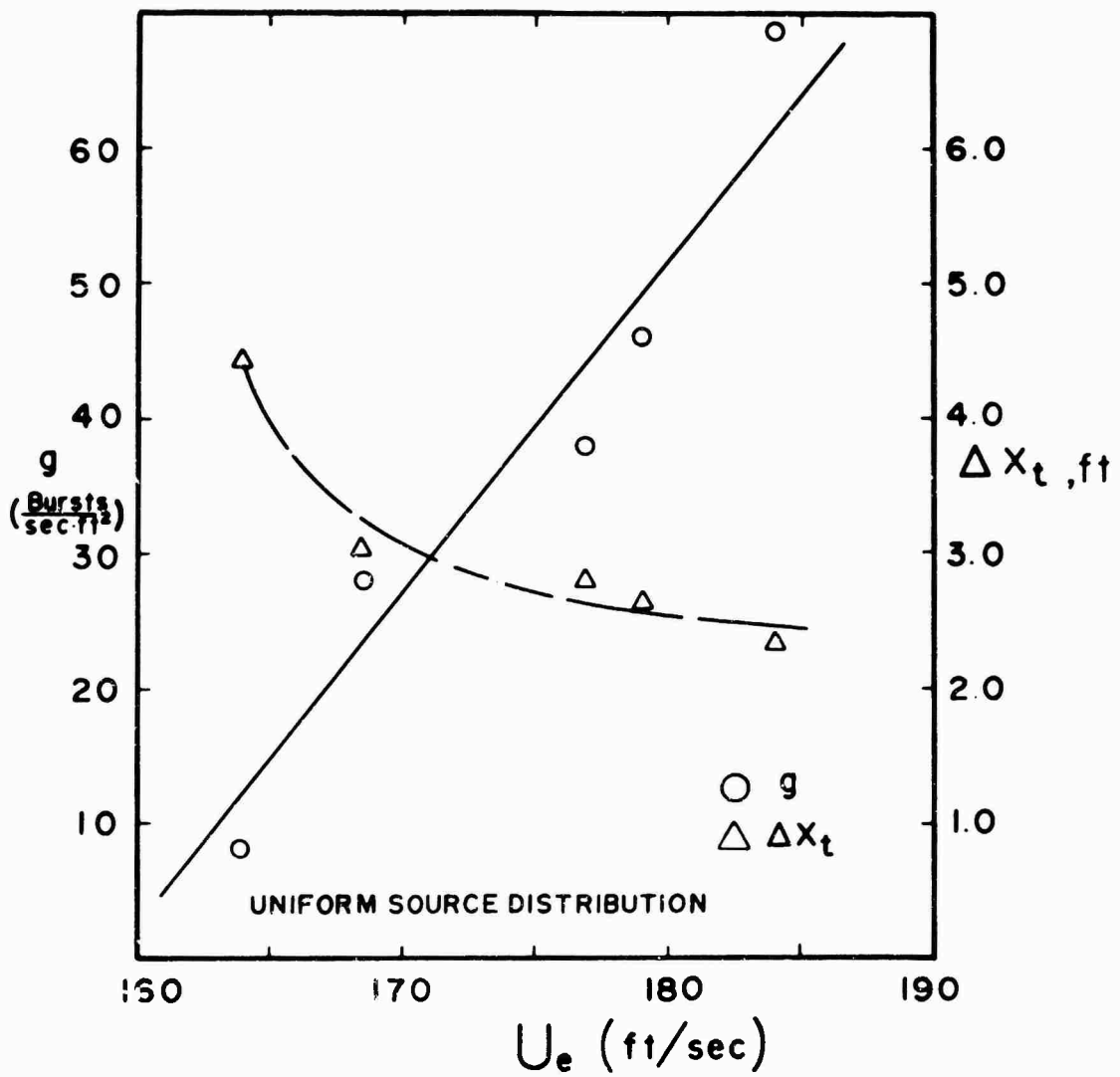


Figure 9 Magnitude of the Source Rate Density g , and the Width of the Transition Region ΔX_t

Table 1 Emmons' Probabilistic Model

ASSUME $g(x_0, z_0, t_0) = g(x_0)$, $\frac{\text{BURSTS}}{\text{SEC} \cdot \text{UNIT AREA}}$

$$\gamma(P) = 1 - \text{EXP} \left[-\frac{\sigma^*}{U_e} \int_0^x g(x_0) (x - x_0)^2 dx_0 \right]$$

$$f_B(P) = \text{TAN } a \int_0^x (x - x_0) g(x_0) \text{EXP} \left[-\frac{\sigma^*}{U_e} \int_0^{x_0} g(x_0') (x - x_0')^2 dx_0' \right] dx_0$$

$$\bar{T}_B(P) = \gamma(P)/f_B(P), \sigma^* = \frac{U_G U_e}{U_c U_t} \text{TAN } a$$

$$g = n\delta(x - x_t)$$

$$\gamma(\bar{x}) = 1 - \text{EXP} [-4.1850 \bar{x}^2]$$

$$\tilde{f}_B(\bar{x}) = 2.0457 \bar{x} \text{EXP} [-4.1850 \bar{x}^2]$$

$$\tilde{f}_B \equiv \frac{f_B}{n \text{TAN } a \sqrt{\frac{U_e}{\sigma^* n}}}$$

$$\bar{x} = \frac{x - x_t}{\Delta x_t}$$

$$\Delta x_t = 2.0457 \sqrt{\frac{U_e}{n\sigma^*}}, \text{ WIDTH OF TRANSITION}$$

$$\tilde{T}_B = \frac{\gamma}{\tilde{f}_B}$$

$$g = \text{CONSTANT}$$

$$\gamma(\bar{x}) = 1 - \text{EXP} [-3.0354 \bar{x}^3]$$

$$\frac{\tilde{f}_B(\bar{x})}{4.3607} = \int_0^{\bar{x}} \zeta \cdot \text{EXP} [3.0354 (\zeta^3 - \bar{x}^3)] d\zeta$$

$$\tilde{f}_B \equiv \frac{f_B}{g \text{TAN } a \left(\frac{U_e}{g\sigma^*}\right)^{2/3}}$$

$$\Delta x_t = 1.4479 \sqrt[3]{\frac{3U_e}{g\sigma^*}}$$

APPENDIX A

DERIVATION OF THE INCREMENTAL VOLUME ELEMENT

Schubauer and Klebanoff³ found the shape of turbulent bursts to be wedge-like pointing downstream. The shape of the Retrograde Cone shown in Figure A1 also forms a wedge like area when projected on the xy plane. The locus of all points P_0 which can influence the state of turbulence at point P forms the volume represented by the Retrograde Cone in Figure A1. If the $x = \text{constant}$ cross section of the cone is approximated by the shape of a triangle the volume element dV_0 in the integral relations (4) and (8) can easily be found.

The volume of the Retrograde Cone for bursts originating at x_0 is given as

$$V = \frac{1}{3} A_b \xi$$

where ξ is the downstream distance from the measurement point, P, to the point of burst origin, P_0 . The area A_b is the projection of the Retrograde Cone on the yt plane at point P_0 . From Figure A1 it is seen that

$$A_b = \frac{1}{2} \tau_{B_{\max}} d$$

where $d = 2\xi \tan(\alpha)$, thus A_b becomes

$$A_b = \xi \tau_{B_{\max}} \tan(\alpha)$$

The relationship for $\tau_{B_{\max}}$ can be shown to be

$$\tau_{B_{\max}} = \frac{U}{U_c} \frac{g}{U_t} \xi$$

thus A_b is then given as

$$A_b = \xi^2 \frac{U_g}{U_c U_t} \tan(\alpha)$$

and the expression for the volume is

$$V = \frac{1}{3} A_b \xi = \frac{\xi^3}{3} \frac{U_g}{U_c U_t} \tan(\alpha)$$

Now defining a propagation parameter, σ^* , as

$$\sigma^* = \frac{U_g U_e}{U_c U_t} \tan(\alpha)$$

we can then express V as

$$V = \frac{\xi^3}{3} \frac{\sigma^*}{U_e}$$

From this relationship the incremental element, dV , of the Retrograde Core, can be expressed as

$$dV = \frac{\sigma^*}{U_e} \xi^2 d\xi$$

In this relationship the ξ variable represents the distance downstream from the transition point, thus in keeping with the nomenclature used in the text the variable ξ is expressed as $x-x_0$, thus we get that

$$dV_0 = \frac{\sigma^*}{U_e} (x-x_0)^2 dx_0$$

APPENDIX B

MEASUREMENT OF INTERMITTENT PRESSURE FIELD PROPERTIES

The fluctuating pressures on the plate surface were measured with Bruel and Kjaer 1/4-inch and 1/8-inch Condenser Microphones. To facilitate the measurement of the pressure on the plate surface over as small an area as possible, the microphones were used with solid protective caps mounted flush with the plate surface and in each of which was drilled a single 1/32-inch diameter hole.

The intermittency factor of the wall pressure field was varied by changing the flow velocity, since the position of the pressure transducers were fixed and could not be varied without stopping the wind tunnel. It is assumed that properties of the intermittent pressure field which are dependent on γ , are independent of whether the intermittency was varied through change of flow velocity U_∞ or change in the streamwise position x in the intermittent region. Inherent in this assumption is the basic assumption that secondary effects on the transition process, such as turbulence intensity, plate vibration, etc., are not altered by the small fractional change in velocity necessary to vary the intermittency factor over its range from 0 to 1, at a fixed point on the surface. The fact that the distributions of the intermittency factor through the intermittent streamwise transition region collapsed well when represented in terms of a normalized Reynolds number (as shown in Figure 3) further substantiates the interchangeability of velocity or streamwise position for this study of the intermittent pressure field.

The intermittent signals from the pressure transducer located in the intermittent transition region of the flat plate boundary layer were displayed on oscillographs. By noting the fraction of the sample time that the oscillograph trace was turbulent the intermittency factor was determined as a function of flow velocity and streamwise distance x from the plate's leading edge. The average burst length and burst frequency were also calculated from the oscillographs. Simultaneous oscillograph traces of the signals from two transducers located on the plate surface with streamwise spatial separations were used to determine the velocities of the leading (downstream) and trailing (upstream) edges of the pressure bursts. Simultaneous oscillographs of signals from transducers separated in the transverse direction to the mean flow were used to determine the width of the bursts and the interior wedge angle θ as shown in Figure 2. These properties of the pressure bursts determined from simultaneous signals of two spatially separated microphones were accomplished by measuring the time differences between the detections of the bursts at the two transducers.

APPENDIX C

METHOD OF NORMALIZATION OF THE DATA

CASE 1 - DIRAC'S DELTA FUNCTION

The statistical relationships which have been derived using a Dirac's Delta Function as the assumed form of the source rate density function are

$$\gamma_1 = 1 - \exp\left[\frac{-\sigma^* n}{U_e} \xi_t^2\right] \quad (16)$$

$$f_B \geq f_{B_1} = n(\tan(\alpha)) \xi_t \exp\left[\frac{-\sigma^* n}{U_e} \xi_t^2\right] \quad (17)$$

and

$$\tau_B = \frac{\gamma(x)}{f_B(x)} \leq \bar{\tau}_{B_1} = \frac{\gamma_1(x)}{f_{B_1}(x)} \quad (18)$$

The streamwise coordinate used in these equations can be selected such that transition occurs at $x = 0$, thus $x_t = 0$ and $\xi_t = x$. This allows the streamwise coordinate to be normalized over the transition region as

$$\bar{x}_1 = \frac{x}{(\Delta x_t)_1} \quad (C1)$$

Equation (21) gives

$$(\Delta x_t)_1 = 2.046 \sqrt{\frac{U_e}{n\sigma^*}} \quad (21)$$

thus

$$\bar{x}_1 = \frac{x}{2.046 \sqrt{\frac{U_e}{n\sigma^*}}} \quad (C2)$$

and

$$0 \leq \bar{x}_1 \leq 1 \quad (C3)$$

Using Equation (C2) we can write

$$x = (2.046) \bar{x}_1 \sqrt{\frac{U_e}{n\sigma^*}} \quad (C4)$$

and Equations (16) and (17) become

$$\gamma_1 = 1 - \exp[-4.185 \bar{x}_1^2] \quad (C5)$$

$$\frac{f_B}{(\Delta x_t)_1} = n \tan(\alpha) 2.046 \sqrt{\frac{U_e}{n\sigma^*}} \bar{x}_1 \exp[-4.185 \bar{x}_1^2] \quad (C6)$$

Equation (C5) is now in normalized form. Table C1.0 shows the values of γ calculated using Equation (C5) for values of $0 \leq \bar{x}_1 \leq 1.1$.

In order to normalize Equation (C6) we define a normalized burst rate frequency \bar{f}_B as

$$\bar{f}_{B_1} \equiv \frac{f_B}{n \sqrt{\frac{U_e}{n\sigma^*}} \tan(\alpha)} = 2.046 \bar{x}_1 \exp[-4.185 \bar{x}_1^2] \quad (C7)$$

Once the relationship between n and U_e is known f_{B_1} can be divided by $n \sqrt{\frac{U_e}{n\sigma^*}} \tan(\alpha)$ to normalize the experimental data for comparison with

the analytical results given by

$$\bar{f}_{B_1} = 2.046 \bar{x}_1 \exp[-4.185 \bar{x}_1^2] \quad (C8)$$

Table C1.0 shows the analytical results found using Equation (C8).

A relationship between n and U_e is determined by setting

$$\bar{f}_{B_1} = \frac{f_B}{n \sqrt{\frac{U_e}{n\sigma^*}} \tan(\alpha)} \quad (C9)$$

equal to the maximum burst rate frequency calculated from Equation (C8). Hence

$$\bar{f}_{B_1 \max} = \frac{f_{B_1 \max}}{n \sqrt{\frac{U_e}{n\sigma^*}} \tan(\alpha)} = .430 \quad (C10)$$

Then we can write

$$f_{B_1 \max} = .430 n \sqrt{\frac{U_e}{n\sigma^*}} \tan(\alpha) \quad (C11)$$

or

$$n = \frac{1}{U_e} \frac{\sigma^* f_{B_1 \max}^2}{[0.430 \tan(\alpha)]^2} \quad (C12)$$

Using the experimentally determined values of $\tan(\alpha)$ and σ^* ,

$\tan(\alpha) = 0.571$, $\sigma^* = 3.327 \tan(\alpha) = 1.898$, Equation (C12) becomes

$$n = 31.165 \frac{f_{B_1 \max}^2}{U_e} \quad (C13)$$

With the experimentally measured values of $f_{B_{\max}}$ at each flow velocity, U_e , it is then possible to determine the relationship between n and U_e . This relation between n and U_e is shown graphically in Figure 8. For simplification a linear relationship between n and U_e is assumed (as shown by the straight line in Figure 8) for normalizing the experimental values of f_B at a given U_e .

Using the relationship between n and U_e the experimental values of f_B are normalized in the form $f_B / n \sqrt{\frac{U_e}{g\sigma^*}} (\tan(\alpha))$ and compared to the normalized analytical results found from Equation (C8). This comparison is shown in Figure 6.

CASE 2 - CONSTANT SOURCE

The normalization process for the Equations where the source rate density function is a constant is the same as in Case 1. The statistical relationships are

$$\gamma^2 = 1 - \exp\left[-\frac{g\sigma^*}{3U_e} \xi_t^3\right] \quad (23)$$

$$f_B \geq f_{B_2} = g \tan(\alpha) \exp\left[\frac{-g\sigma^*}{3U_e} \xi_t^3\right] \int_0^{\xi_t} \zeta \exp\left[\frac{g\sigma^*}{3U_e} \zeta^3\right] d\zeta \quad (24)$$

$$\tau_B = \frac{Y(x)}{f_B(x)} \leq \bar{\tau}_{B_2} = \frac{Y_2(x)}{f_{B_2}(x)} \quad (25)$$

The normalization process of the streamwise coordinate, x , is similar to that in Case 1. In this manner the relation

$$(\Delta x_t)_2 = 1.448 \sqrt[3]{\frac{3U_e}{g\sigma^*}} \quad (27)$$

is used to yield a relation for the normalized coordinate \bar{x}_2 ,

$$x = \bar{x}_2 \cdot 1.448 \sqrt[3]{\frac{3U}{g\sigma^*}} \quad (C14)$$

where again

$$0 \leq \bar{x}_2 \leq 1. \quad (C15)$$

Using the normalized coordinate in Equations (23) and (24) gives

$$\gamma_2 = 1 - \exp[-3.035 \bar{x}_2^3] \quad (C16)$$

$$f_{B_2} = 4.361 g(\tan(\alpha)) \left[\frac{U}{g\sigma^*}\right]^{2/3} \int_0^{\bar{x}_2} \zeta \exp[3.035(\zeta^3 - \bar{x}_2^3)] d\zeta \quad (C17)$$

Equation (C16) is now in normalized form. Table C1.1 shows the values of γ calculated using Equation (C16) for values of $0 \leq \bar{x}_2 \leq 1.1$.

To normalize Equation (C17) we define a normalized burst rate frequency \bar{f}_{B_2} as

$$\bar{f}_{B_2} = \frac{f_{B_2}}{g \tan(\alpha) \left[\frac{U}{g\sigma^*}\right]^{2/3}} = 4.361 \int_0^{\bar{x}_2} \zeta \exp[3.035(\zeta^3 - \bar{x}_2^3)] d\zeta \quad (C18)$$

The right hand side of Equation (C18)

$$\bar{f}_{B_2} = 4.361 \int_0^{\bar{x}_2} \zeta \exp[3.035(\zeta^3 - \bar{x}_2^3)] d\zeta \quad (C19)$$

is the normalized analytical result. Table C1.1 shows the analytical results found using Equation (C19). The left hand side of Equation (C18) gives a relation for normalizing the experimental results,

$$\bar{f}_{B_2} = \frac{f_B^2}{g \tan(\alpha) \left[\frac{U_e}{g \sigma^*} \right]^{2/3}} \quad (C20)$$

Once the relationship between g and U_e is known, Equation (C20) can be used to normalize the experimental data thus allowing a direct comparison between the normalized analytical results (Equation (C19)) and the normalized experimental results (Equation (C20)).

A relationship between g and U_e is obtained by setting Equation (C20) equal to the maximum burst rate frequency calculated from Equation (C19)

$$\bar{f}_{B_2} = \frac{f_{B_{2max}}^2}{g \tan(\alpha) \left[\frac{U_e}{g \sigma^*} \right]^{2/3}} = 0.618 \quad (C21)$$

From Equation (C21) we can write

$$g = \frac{f_{B_{2max}}^3 \sigma^{*2}}{U_e^2 (0.618 \tan(\alpha))^3} \quad (C22)$$

then using the experimentally determined values of $\tan(\alpha)$ and σ^* we get

$$g = 82.202 \frac{f_{B_{2max}}^3}{U_e^2} \quad (C23)$$

With the experimentally measured values of $f_{B_{\max}}$ it is therefore possible to determine a relationship between g and U_e . This relationship between n and U_e is shown in Figure 9.

Knowing the relationship between g and U_e , it is then possible to normalize the experimental data, using Equation (C20), and compare it to the normalized analytical results found from Equation (C19). This comparison is shown in Figure 7. Again, a simple linear relationship (shown on the figure) was used for normalizing the experimental values of f_B at a given U_e .

TABLE C1.0
 NORMALIZED ANALYTIC RESULTS

$$g = n\delta(x-x_t)$$

\bar{x}_1	γ_1	f_{B_1}	$\bar{\tau}_{B_1}$
.05	.01041	.10122	.10282
.10	.04986	.19619	.20892
.15	.08987	.27928	.32178
.20	.15414	.34608	.44539
.25	.23015	.39372	.58456
.30	.31384	.42110	.74529
.35	.40110	.42881	.93538
.40	.48809	.41889	1.16520
.45	.57150	.39446	1.44880
.50	.64875	.35928	1.80570
.55	.71803	.31725	2.26329
.60	.77834	.27207	2.86077
.65	.82935	.22691	3.65500
.70	.87135	.18423	4.72975
.75	.90502	.14573	6.21027
.80	.93133	.11239	8.2868
.85	.95138	.08455	11.25257
.90	.96629	.06207	15.56734
.95	.97711	.04449	21.96296
1.00	.98478	.03114	31.62414
1.05	.99009	.02129	46.50084
1.10	.99368	.01422	69.85757

TABLE C1.1
 NORMALIZED ANALYTIC RESULTS

g = constant

x_2	γ_2	f_{B_2}	$\bar{\tau}_{B_2}$
.05	.00038	.00545	.06961
.10	.00303	.02176	.13925
.15	.01019	.04876	.20904
.20	.02399	.08596	.27910
.25	.04632	.13247	.34967
.30	.07869	.18689	.42103
.35	.12203	.24722	.49361
.40	.17656	.31101	.56771
.45	.24164	.37531	.64385
.50	.31575	.43697	.72258
.55	.39650	.49286	.80449
.60	.48089	.54020	.89022
.65	.56552	.57682	.98040
.70	.64695	.60145	1.07565
.75	.72212	.61378	1.17652
.80	.78863	.61450	1.28337
.85	.84500	.60513	1.39634
.90	.89061	.58779	1.51518
.95	.92591	.56484	1.63925
1.00	.95194	.53859	1.76748
1.05	.97022	.51106	1.89844
1.10	.98240	.48382	2.03052

LIST OF FIGURES

	Page
Figure A1 <u>Retrograde Cone Region R</u> Cone-like Volume of all Points P which can Influence the State of Turbulence at Point P	31

LIST OF TABLES

Table C1.0 Normalized analytic results $g = n\delta(x-x_t)$	41
Table C1.1 Normalized analytic results $g = \text{constant}$	42

REFERENCES

1. Emmons, H.W., "The Laminar-Turbulent Transition in a Boundary Layer - Part I," J. Aero. Sci., 18, 490, 1951.
2. Emmons, H.W. and Bryson, A.E., "The Laminar-Turbulent Transition in a Boundary Layer - Part II," Proceedings of the First U.S. National Congress of Theoretical and Applied Mechanics, 859, 1952
3. Schubauer, G.B. and Klebanoff, P.S., "Contributions on the Mechanics of Boundary Layer Transition," National Advisory Committee for Aeronautics Report No. 1289, 1956
4. DeMetz, F.C. and Casarella, M.J., "An Experimental Study of the Intermittent Properties of the Boundary Layer Pressure Field During Transition on a Flat Plate," NSRDC Report No. 4140, Nov 1973
5. Brownell, W.F., "An Anechoic Flow Facility Design for Naval Ship Research and Development Center, Carderock," NSRDC Report No. 2924 Sep 1968
6. Jorgensen, D.W., Casarella, M.J. and Shen, J.T.C., "The Design and Application of a Test Fixture for Flow Noise Measurements in the Anechoic Test Facility," NSRDC Report No. SAD-374-942, Dec 1970
7. Narasimha, R., "On the Distribution of Intermittency in the Transition Region of a Boundary Layer," J. Aero. Sci., 24, 711, 1957
8. Schubauer, G.B. and Skramstad, H.K., "Laminar Boundary Layer Stability and Transition on a Flat Plate," National Advisory Committee for Aeronautics Report No. 909, 1943